

Evasive ice X and heavy fermion ice XII: facts and fiction about high-pressure ices

W.B. Holzapfel*

Fachbereich Physik, Universität-GH Paderborn, D-33095 Paderborn, Germany

Abstract

Recent theoretical and experimental results on the structure and dynamics of ice in wide regions of pressure and temperature are compared with earlier models and predictions to illustrate the evasive nature of ice X, which was originally introduced as completely ordered form of ice with short single centred hydrogen bonds isostructural Cu_2O . Due to the lack of experimental information on the proton ordering in the pressure and temperature region for the possible occurrence of ice X, effects of thermal and quantum delocalization are discussed with respect to the shape of the phase diagram and other structural models consistent with present optical and X-ray data for this region. Theoretical evidences for an additional orthorhombic modification (ice XI) at higher pressures are confronted with various reasons supporting a delocalization of the protons in the form of a heavy fermion system with very unique physical properties characterizing this fictitious new phase of ice XII. © 1999 Elsevier Science B.V. All rights reserved.

Keywords: Ices; Hydrogen bonds; Phase diagram; Equation of states

1. Introduction

The first in situ X-ray studies on H_2O and D_2O ice VII under pressures up to 20 GPa [1] together with a simple twin Morse potential (TMP) model for protons or deuterons in hydrogen bonds [2] allowed almost 26 years ago first speculations about a very special phase of ice with symmetric monomodal hydrogen bonds, which was proposed to occur at pressures of about 50 GPa with an uncertainty of + 40 GPa or – 15 GPa, depending on the contribution from zero-point motion and

tunnelling [2]. Detailed Raman studies on H_2O and D_2O ice VIII to pressures in the range of 50 GPa [3] revealed the expected softening in the molecular stretching modes and led to the determination of a critical O–H–O bond length of $R_c = 232$ pm, where the central barrier of the effective double-well potential should disappear [4]. If the ice rules [5] would still be obeyed, the tetragonally distorted structure tI24 of hydrogen ordered ice VIII should thereby transform into cP6 ice X, a hydrogen ordered cubic structure of Cu_2O -type (structures are labelled with Pearson symbols according to Ref. [6]). Later theoretical [7] and experimental [8] studies revealed that tunnelling-induced disorder [9] interferes with this direct transition from ordered tI24 ice VIII to ordered

* Fax: + 49-5251-6037-38; e-mail: holz-we@physik.uni-paderborn.de.

cP6 ice X by the extension of the disordered phase ice VII with its average $\overline{\text{cI6}}$ structure to very low temperatures just in the pressure range, where ice X was expected to occur as illustrated in Fig. 1.

These observations led to the question, whether an ordered phase ice X ever occurs and how one could find a (thermodynamic) phase boundary between the disordered $\overline{\text{cI6}}$ ice VII and the ordered cP6 ice X, considering that the precise dynamical disorder in ice VII at low pressures is even not yet clear [27,28].

Also the high-pressure Raman [3,4,29–33] and IR studies [34–39] have not yet allowed to locate the ice VII–X phase boundary precisely. A linear extrapolation of the classical softmode behaviour [40] observed at lower pressures [3,4,29–39] is certainly not appropriate for the motion of protons or deuterons when tunnelling becomes important as illustrated recently [41]. In fact, the first discussions of this soft-mode behaviour [4] treated the proton and deuteron motions much more appropriately with a quantum mechanical model than the later semi-classical models [29–38]. However,

an effective simple Morse potential had to be used initially [4] due to the fact that this simple model gave fully analytical results and the more advanced computer codes [41] were not yet available.

All the extrapolations of these results into the region, where the ice VII–X transition is expected to occur, did not really allow to locate the transition. In fact, also the recent publication on ‘Cascading Fermi Resonances and the Soft-Mode in Dense Ice’ [38] used for the evaluation of the spectra in the transition region only the classical soft-mode picture and different interpretations of these data appear to be more reasonable [41].

Therefore, the question remained, whether studies on the equation of state (EOS) of ice VII might give some hints for the location of the ice VII–X transition.

2. Analysis of EOS data

The compilation of all the EOS data for H_2O -ice VII in Fig. 2 illustrates first of all, that all the data

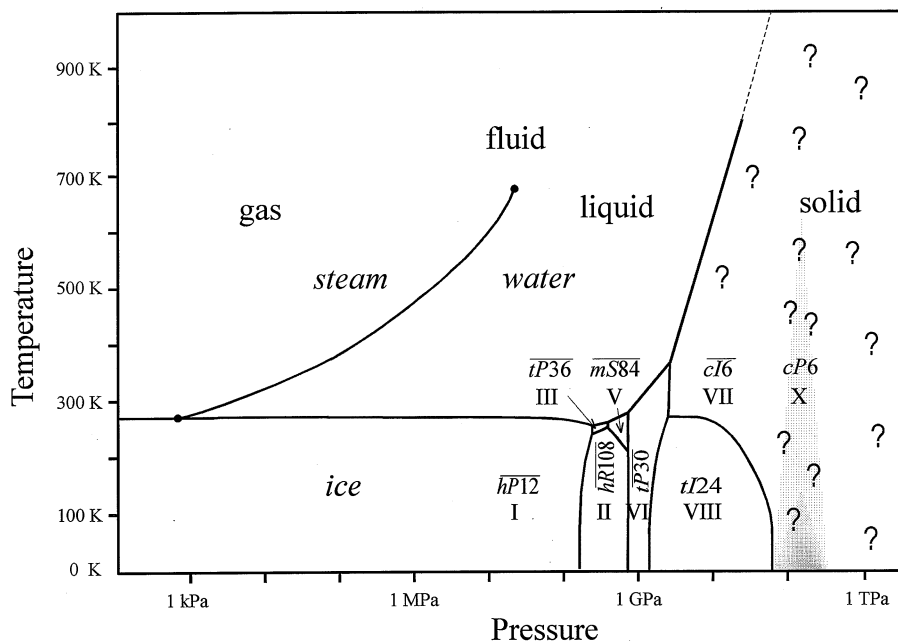


Fig. 1. Thermodynamic phase diagram for H_2O ices based on various data from the literature [10–26]. The different stable phases of ice are labelled with the commonly used roman numbers and also with Pearson symbols [6], which are overlined, when an average structure with hydrogen disordered is represented.

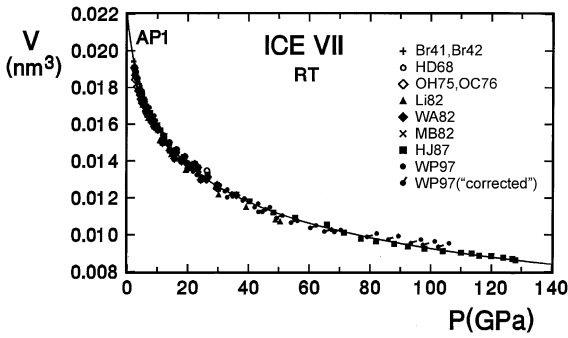


Fig. 2. P - V data for ice VII at room temperature from direct volume measurements at low pressures [13,14] and different X-ray diffraction studies at higher pressures [1,29,42–47].

together [1,13,14,29,42–47] are well represented just by one smooth curve labelled AP1 in Fig. 2. In fact, the same curve AP1 also fits similarly well all the data [1,45,47] for D_2O -ice VII. Therefore, these data are not shown separately here. A more detailed insight into possible slight anomalies in such data is commonly obtained by the use of various ‘linearization schemes’ [48–57]. However, spurious phase transitions have been derived by these procedures especially for ice [47,58,59] as one can notice by inspection of all the ‘linearized’ data in Fig. 3, where these spurious ‘anomalies’ disappear just in the spread of the experimental uncertainties. Obviously, a large scattering of the data can be noticed in this plot. To a large extent, deviatoric (non-hydrostatic) stresses can easily explain this scattering. Some authors tried to correct their data for these effects [47] and these ‘corrected’ data show indeed better agreement with the average interpolating curve AP1. However, even these corrections must be treated with much caution, since (a) only a uniaxial stress component was taken into account [47] but no elastic inhomogeneity between the sample and the ruby (Lamé pressure [60]), (b) the Singh-Kennedy effect [61] was evaluated with the assumption of a pure Voigt case (strain continuity at the grain boundaries), and (c), in contrast to the ruby calibration and all previous definitions, the hydrostatic pressure was evaluated by subtraction of a uniaxial component, whereas the usual definition takes deviatoric stresses already into account [61].

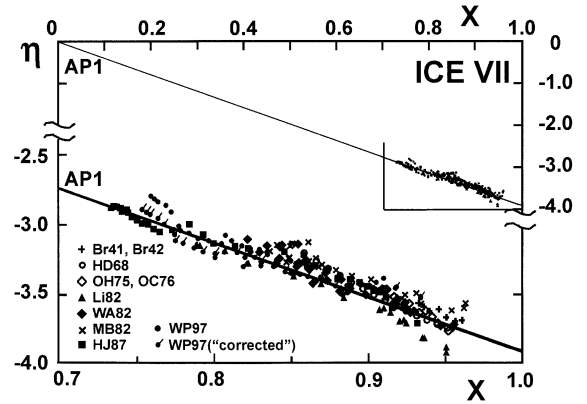


Fig. 3. η - x -scaling of the P - V data for ice VII at room temperatures. Thereby, $x = (V/V_0)^{1/3}$ and $\eta = \ln((P/P_{FG0})x^5/(1-x))$ with $V_0 = 0.0214 \text{ nm}^3$ for the effective molecular volume at 0 GPa and the corresponding Fermi gas pressure $P_{FG0} = a_{FG}(Z/V_0)$ with $a_{FG} = 23.37 \text{ MPa nm}^5$ and $Z = 10$ for the water molecule. AP1 represents a linear interpolation to very high compression for a ‘simple’ solid as shown in the upper part of this diagram.

In short, the shift of the corrected data [47] gives only a rough estimate for the uncertainty in this correction and illustrates that in this case as well as in the previous discussions [58,59] of earlier X-ray data [44,46] only spurious anomalies due to varying deviatoric stresses were taken just too seriously. Also Brillouin scattering data [62–65] do not find these spurious anomalies. Therefore, no clear evidence for a sharp ice VII–X transition can be derived from any of these data yet. Therefore, one may consider that model calculations can possibly give some further hints for the characterization of this ‘evasive’ phase transition.

3. Model calculations

After the early semiempirical prediction of a possible transition of either $c16$ ice VII or $tP12$ ice VIII into a highly symmetric form [2], later labelled [4,62] ice X, modelling of this transition was performed at various different levels of sophistication [7,66–77]. If thereby the ground state as well as the dynamics of hydrogen (and oxygen) motion are treated quantum mechanically [7,66,69,70,76,77] tunneling induced disorder [9] is found to drive the

transition from ice VIII to ice VII at zero temperature at a critical pressure P_c , which depends on the isotopic mass and is slightly lower than the expected pressure for the occurrence of ‘ordered’ ice X. However, the exact nature of the ice VII–X transition still seems to need some clarification.

Since the application of a ‘generalized’ double Morse potential (DMP) [41] led to a much better understanding of the effects of pressure on the IR

and Raman data for ice and other hydrogen-bonded systems [41,78], the same potential was used in the present study to gain more insight into the structural changes and hydrogen dynamics of ice in the range of the expected ice VII–X transition as illustrated in Fig. 4 by a few ‘effective’ hydrogen potential surfaces projected onto a (0 1 1) plane of the BCC oxygen lattice together with a few projections of the corresponding barriers E_H and E_P for

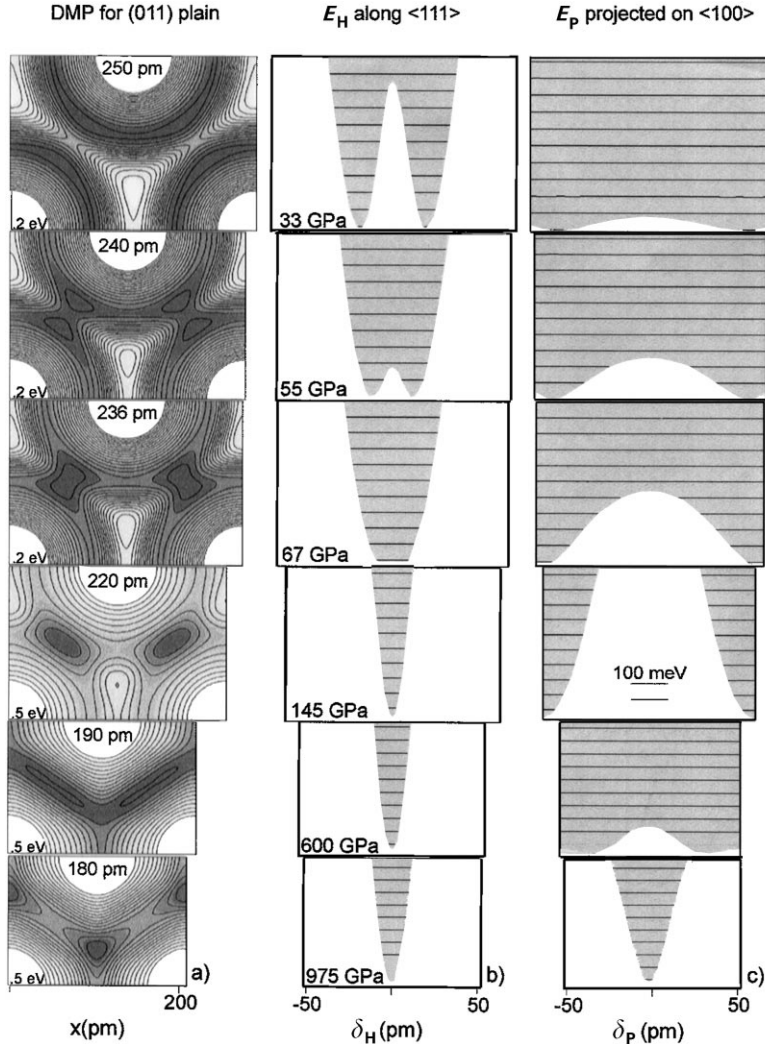


Fig. 4. Effective hydrogen model potentials at different pressures for a BCC oxygen lattice based on a generalized Double Morse Potential (DMP) using the parameter set 1 [41]. (a) Potential surface projected on to the (0 1 1) plane. The corresponding H-bond length R is given on each plot together with the energy difference between adjacent contour lines. (b) Potential barrier E_H along $\langle 111 \rangle$ H-bond directions δ_H . Horizontal lines denote energy differences of 100 meV and the corresponding pressures are also indicated. (c) Potential barrier E_P for the valley between $\langle 111 \rangle$ and $\langle 1\bar{1}\bar{1} \rangle$ directions.

the hydrogen motion along the H-bond directions and perpendicular to them. It should be kept in mind, that these potential surfaces, like muffin-tin potentials for conduction electrons, do not take into account individual hydrogen–hydrogen interactions or correlations, but they are useful to study the quantum effects related to the hydrogen delocalization. Therefore, the barrier E_p for molecular rotations is unrealistically low at moderate pressures or, in other words, for large values of the hydrogen bond length R_{00} as illustrated in Fig. 5. However, the strong stiffening of the rotational and librational motions [3,34–38] is modelled rather reasonably by the strong increase of E_p until a new decrease heralds a lattice instability at several hundreds GPa. In contrast to the earlier simple TMP model [2], the parameter set 1 for this DMP [41] reproduces very reasonably the weak variations of

the oxygen–deuteron distance R_{OD} measured with neutron diffraction on ice VIII under pressure [72,79–81]. Effects of zero-point motion (or QM delocalization) account for the difference between the location of the minimum R_{OM} and the measured positions R_{OD} . The larger values for hydrogen bond distances R_{OH} calculated by a fully quantum mechanical path integral technique [77] illustrate even more clearly the spread of the proton wave function, which was modelled in a similar way also with the present potential [41]. In fact, a qualitative plot of the proton zero-point energy E_0 in Fig. 5, estimated from the previous calculations [41], illustrates also here, that the tunnelling-induced disorder must be expected already at $R_{00} \approx 240$ pm, which corresponds to a pressure of about 55 GPa, if one uses the EOS AP1 from Fig. 2. This close agreement with the experimental value of 64 GPa

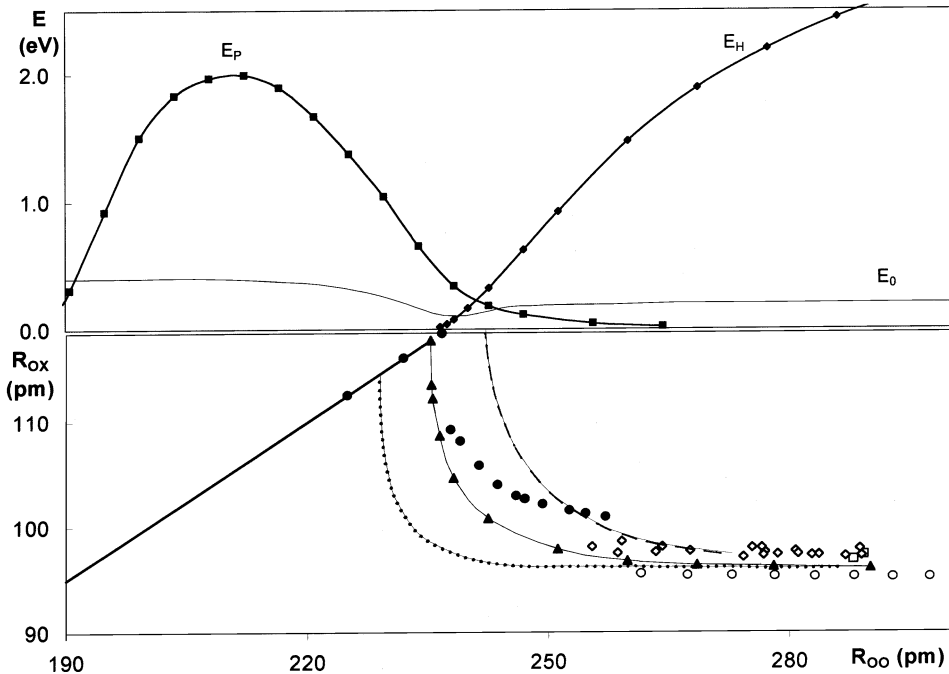


Fig. 5. Variation of the barrier the height E_H and E_p from Fig. 4 and zero-point energy E_0 for protons estimated from the DMP calculations [41]. The corresponding location of the potential minimum R_{OM} on the bond versus bond length R_{00} is also shown by the thin continuous line in the lower part. Similar variations of R_{OM} for the parameter set 2 [41] and for a new parameter set 3 of the same DMP model [41] are also indicated by dashed and dotted lines, respectively, together with data from ab initio Hartree–Fock calculations [72] reproduced by open circles. Results for the proton position from ab initio modelling [77] including zero-point motion are illustrated by solid dots. Deuteron positions from early [5,27] and more recent [72,79–81] high-pressure neutron diffraction on ice VIII are shown by open squares and diamonds, respectively.

[8] is obviously fortuitous as illustrated with the parameter set 2 [41] and a similarly modified parameter set 3 in Fig. 5.

Certainly, a fine tuning of this DMP could be performed in the future to account more precisely for the experimental facts, however, even the present form points with the very strong decrease of E_p at $R_{00} < 210$ pm, or $P > 230$ GPa to an interesting feature illustrated in Fig. 4 by the extended flat valley of the potential in the (0 1 1) plane. If the BCC oxygen lattice remains stable up to this pressure, this flat potential and the high zero-point energy of the protons would probably lead to a delocalization of the protons in a half-filled ‘proton band’ with the possible occurrence of ‘metallic’ proton conduction with minor electronic contributions. This extraordinary state of a degenerate Fermi gas of protons or deuterons in a stable oxygen lattice could be considered as a new form of ‘heavy fermion’ ice XII.

4. Conclusions

All the presently available experimental and theoretical data indicate, that the ‘phase transition’ ice VII–X is neither first nor second order but rather ‘continuous’ in such a way that no thermodynamic discontinuity but only an arbitrary definition or extrapolation can possibly locate the corresponding ‘transition line’ in the P – T phase diagram.

Similarly, various ‘phase transitions’ in the stability range of ice VII may be related only to rather smooth structural changes from molecular disorder at low pressures to thermally activated dissociation at intermediate pressures and tunnelling-induced disorder at higher pressures (and low temperatures) before most of the disorder is squeezed out in the stability range of ice X. At elevated temperatures, the gradual change from orientational disorder in the initially molecular structure to predominantly ‘ionic’ disorder along the bonds with minor violations of the ice rules could smoothly turn over into a different kind of disorder disturbing the tetrahedral hydrogen arrangement typical for cP6 ice X. This different form of cI6 ice VII with monomodal H-bonds but strong proton or deuteron hopping between the eight equivalent ($\pm \frac{1}{4}$, $\pm \frac{1}{4}$ $\pm \frac{1}{4}$) sites

could show at first superionic conduction but finally also a Mott-transition of the protons or deuterons into a heavy fermion state, resulting in an ordered structure cI6 ice XII, if the BCC oxygen lattice remains stable. Even if denser oxygen packing and low symmetry structures [58,68,69,73,82] may suppress the occurrence of such a state at low temperatures, it is conceivable that the BCC oxygen lattice could be stabilized as a high-temperature phase due to its softer phonons and additional entropy from the proton disorder.

With respect to this question it would be interesting to see, whether the same kind of orthorhombic high-pressure phase predicted and labelled as ice XI [73] would also be predicted for Cu_2O and Ag_2O under pressure, where different structures have been found experimentally [83].

On the other hand, one can conceive also that the molecular disorder typical for cI6 ice VII at low pressures changes gradually to a different type of disorder cP6 ice VII, which may still satisfy the ice rules perfectly in the form of an average cupric structure, however, with thermal- or tunnelling-induced disorder resulting in a bimodal distribution of the hydrogens along the bonds, keeping the (slightly distorted) tetrahedral arrangement of the hydrogens with only a minor number of defect H-positions occupied. In principle, these two types of different proton disorder, cI6 and cP6, and a third type of hydrogen disorder in cI6 with a monomodal half occupation of the 8 ($\pm \frac{1}{4} \pm \frac{1}{4} \pm \frac{1}{4}$) sites should be distinguishable by X-ray diffraction, and also with respect to ordered cP6 ice X. While the oxygen-dominated reflections occur in all these four structures, in a similar way (condition on hkl : $h + k + l = 2n$) very weak additional H-dominated reflections are expected for cP6 ice X (all h, k, l odd!). For the bimodal distribution in (disordered) cP6 additional weak reflections with one odd and two even values ($\neq 0$) in h, k, l would be allowed, in the monomodal disordered structure cI6 only these later H-dominated reflections should be present besides the regular BCC reflections, and in the bimodally disordered cI6 ice VII only these oxygen-dominated BCC reflections should be seen. However, this distinction depends

on the intensity of the very weak H-dominated reflections, which could be broadened also depending on the extent of the disorder. Furthermore, the approach towards the monomodal H-distribution is certainly smeared out by the coupling of the hydrogen location to the oxygen motion, which results in additional disorder and uncertainty in the approach towards the ordered cP6 ice X structure with its definite monomodal H-distribution.

All these considerations indicate that ‘phase boundaries’ between the two forms of ideally disordered cI6 ice and the ordered cP6 ice X may not exist in a macroscopic (thermodynamic) sense, but may be defined only by (artificial) selection of some specific microscopic criteria or by correspondingly artificial (extrapolation) procedures applied to experimental data.

In addition, similar continuous changes as proposed here for ice VII are obviously noticed in electrical conductivity measurements on fluid water under high pressure [84–87] showing at first a strong increase related to molecular dissociation and extra mobility of the hydrogen ions but finally a saturation of the conductivity at 30 GPa [87], where the rotational barrier E_p becomes comparable to the activation energy for dissociation related to E_H .

Finally, it is conceivable that hydrogen delocalization into a heavy fermion state has already been observed experimentally under pressure in conductivity measurements on solid H₂S [88].

Acknowledgements

Stimulating discussions with P.G. Johannsen, strong support in the model calculations by M. Hartwig, and much patience in the typesetting of the manuscript by S. Weeke are gratefully acknowledged.

References

- [1] W.B. Holzapfel, H.G. Drickamer, *J. Chem. Phys.* 48 (1968) 4798.
- [2] W.B. Holzapfel, *J. Chem. Phys.* 56 (1972) 712.
- [3] K.R. Hirsch, W.B. Holzapfel, *J. Chem. Phys.* 84 (1986) 2771.
- [4] R. Hirsch, W.B. Holzapfel, *Phys. Lett.* 101A (1984) 142.
- [5] J.D. Jorgensen, R.A. Beyerlein, N. Watanabe, T.G. Worlton, *J. Chem. Phys.* 81 (1984) 3211.
- [6] G.J. Leigh (Ed.), *Nomenclature of Inorganic Chemistry, International Union of Pure and Applied Chemistry, Recommendations 1990*, Blackwell, Oxford, 1990.
- [7] K.S. Schweizer, F.H. Stillinger, *J. Chem. Phys.* 80 (1984) 1230.
- [8] Ph. Pruzan, J.C. Chervin, B. Canny, *J. Chem. Phys.* 99 (1993) 9842.
- [9] R.M. Stratt, *J. Chem. Phys.* 84 (1986) 2315.
- [10] P.W. Bridgman, *Proc. Am. Acad. Arts Sci.* 47 (1912) 441.
- [11] P.W. Bridgman, *J. Chem. Phys.* 3 (1935) 597.
- [12] P.W. Bridgman, *J. Chem. Phys.* 5 (1937) 964.
- [13] P.W. Bridgman, *Proc. J. Chem. Phys.* 9 (1941) 794.
- [14] P.W. Bridgman, *Proc. Am. Acad. Arts Sci.* 74 (1942) 399.
- [15] G.C. Kennedy, P.N. LaMori, *J. Geophys. Res.* 67 (1962) 851.
- [16] C.W.F.T. Pistorius, M.C. Pistorius, J.P. Blakey, L.J. Admiral, *J. Chem. Phys.* 38 (1963) 600.
- [17] J.E. Bertie, E. Whalley, *J. Chem. Phys.* 40 (1964) 1646.
- [18] A.J. Brown, E. Whalley, *J. Chem. Phys.* 45 (1966) 4360.
- [19] E. Whalley, D.W. Davidson, J.B.R. Heath, *J. Chem. Phys.* 43 (1966) 3976.
- [20] J.E. Bertie, *Appl. Spectrosc.* 22 (1968) 634.
- [21] C.W.F.T. Pistorius, E. Rapoport, J.B. Clark, *J. Chem. Phys.* 48 (1968) 5509.
- [22] W.B. Holzapfel, *High Temp.-High Pressure* 1 (1969) 675.
- [23] E. Whalley, O. Mishima, Y.P. Handa, D.D. Klug, *Annals New York Acad. of Sci.* 484 (1986) 81.
- [24] D.D. Klug, Y.P. Handa, J.S. Tse, E. Whalley, *J. Chem. Phys.* 90 (1989) 2390.
- [25] W. Wagner, A. Saul, A. Pruss, *J. Phys. Chem. Ref. Data* 23 (1994) 515.
- [26] F. Datchi, P. Loubeyre, R. LeToullec, *Rev. High Pressure Sci. Technol.* 7 (1998) 778.
- [27] W.F. Kuhs, J.L. Finney, C. Vettier, D.V. Bliss, *J. Chem. Phys.* 81 (1984) 3612.
- [28] R.J. Nelmes, J.S. Loveday, W.G. Marshall, G. Hamel, J.M. Besson, S. Klotz, *Phys. Rev. Lett.* 81 (1998) 2719.
- [29] G.E. Walrafen, M. Abebe, F.A. Mauer, S. Block, G.J. Piermarini, R. Munro, *J. Chem. Phys.* 77 (1982) 2166.
- [30] Ph. Pruzan, J.C. Chervin, M. Gauthier, *Europhys. Lett.* 13 (1990) 81.
- [31] Ph. Pruzan, *J. Mol. Struct.* 322 (1994) 279.
- [32] J.M. Besson, M. Kobayashi, T. Nakai, S. Endo, Ph. Pruzan, *Phys. Rev. B* 55 (1997) 11191.
- [33] Ph. Pruzan, E. Wolanin, M. Gauthier, J.C. Chervin, B. Canny, D. Häusermann, M. Hanfland, *J. Phys. Chem. B* 101 (1997) 6230.
- [34] W.B. Holzapfel, B. Seiler, M.F. Nicol, *J. Geophys. Res.* B 89 (1984) 707.
- [35] K. Aoki, H. Yamawaki, M. Sakashita, *Science* 268 (1995) 1322.
- [36] K. Aoki, H. Yamawaki, M. Sakashita, H. Fujihisa, *Phys. Rev. B* 54 (1996) 15673.
- [37] A.F. Goncharov, V.V. Struzhkin, M.S. Somayazulu, R.J. Hemley, H.K. Mao, *Science* 273 (1996) 218.

- [38] V.V. Struzhkin, A.F. Goncharov, R.J. Hemley, H.K. Mao, *Phys. Rev. Lett.* 78 (1997) 4446.
- [39] H. Yamawaki, M. Sakashita, H. Fujihisa, K. Aoki, *Rev. High Pressure Sci. Technol.* 7 (1998) 1135.
- [40] W.F. Sherman, *J. Phys. C* 15 (1982) 9.
- [41] P.G. Johansson, *J. Phys.: Condens. Matter* 10 (1998) 2241.
- [42] B. Olinger, P.M. Halleck, *J. Chem. Phys.* 62 (1975) 94.
- [43] B. Olinger, H. Cady, in: *Proc. 6th Symp. on Detonation*, Corondado, CA (Office of Naval Research, Arlington, Virginia, report Number ACR-221, 1976) p. 700.
- [44] Lin-gun Liu, *Earth Planetary Sci. Lett.* 61 (1982) 359.
- [45] R.G. Munro, S. Block, F.A. Mauer, G. Piermarini, *J. Appl. Phys.* 53 (1982) 6174.
- [46] R.J. Hemley, A.P. Jephcoat, H.K. Mao, C.S. Zha, L.W. Finger, D.E. Cox, *Nature* 330 (1987) 737.
- [47] E. Wolanin, Ph. Pruzan, J.C. Chervin, B. Canny, M. Gauthier, D. Häusermann, M. Hanfland, *Phys. Rev. B* 56 (1997) 5781.
- [48] H. Schlosser, J. Ferrante, *J. Phys. Chem. Solids* 52 (1991) 635.
- [49] G. Queisser, W.B. Holzapfel, *Appl. Phys. A* 53 (1991) 114.
- [50] W.B. Holzapfel, T. Krüger, W. Sievers, V. Vijayakumar, *Jpn. J. Appl. Phys.* 32 (Suppl. 1) (1993) 16.
- [51] Y.K. Vohra, W.B. Holzapfel, *High Pressure Res.* 11 (1993) 223.
- [52] W.B. Holzapfel, *Physica B* 190 (1993) 21.
- [53] Y.C. Zhao, F. Porsch, W.B. Holzapfel, *Phys. Rev. B* 50 (1994) 6603.
- [54] M. Winzenick, V. Vijayakumar, W.B. Holzapfel, *Phys. Rev. B* 50 (1994) 12381.
- [55] W.B. Holzapfel, *Rep. Prog. Phys.* 59 (1996) 29.
- [56] M. Winzenick, W.B. Holzapfel, in: W. Trzeciakowski (Ed.), *High Pressure Science and Technology*, World Scientific, Singapore, 1996, pp. 384–386.
- [57] W.B. Holzapfel, *High Pressure Res.* 16 (1998) 81.
- [58] J. Hama, K. Suito, in: N. Maeno, T. Hondoh (Eds.), *Physics and Chemistry of Ice*, Hokkaido University Press, Sapporo, 1992, pp. 75–82.
- [59] J. Hama, K. Suito, *Phys. Lett. A* 187 (1994) 346.
- [60] Y. Wang, D.J. Weidner, Y. Meng, in: M.H. Manghnani, T. Yagi (Eds.), *Properties of Earth and Planetary Materials at High Pressure and Temperature*, American Geophysical Union, Washington, 1998, p. 365.
- [61] A.K. Singh, G.C. Kennedy, *J. Appl. Phys.* 45 (1974) 4686.
- [62] A. Polian, M. Grimsditch, *Phys. Rev. Lett.* 52 (1984) 1312.
- [63] H. Shimizu, M. Ohnishi, S. Sasaki, Y. Ishibashi, *Phys. Rev. Lett.* 74 (1995) 2820.
- [64] H. Shimizu, T. Nabetani, T. Nishiba, S. Sasaki, *Phys. Rev. B* 53 (1996) 6107.
- [65] C.S. Zha, H.K. Mao, R.J. Hemley, T.S. Duffy, *Rev. High Pressure Sci. Technol.* 7 (1998) 739.
- [66] F.H. Stillinger, K.S. Schweizer, *J. Phys. Chem.* 87 (1983) 4281.
- [67] P. Demontis, R. LeSar, M.L. Klein, *Phys. Rev. Lett.* 60 (1988) 2284.
- [68] P. Demontis, M.L. Klein, R. LeSar, *Phys. Rev. B* 40 (1989) 2716.
- [69] C. Lee, D. Vanderbilt, K. Laasonen, R. Car, M. Parrinello, *Phys. Rev. Lett.* 69 (1992) 462.
- [70] C. Lee, D. Vanderbilt, K. Laasonen, R. Car, M. Parrinello, *Phys. Rev. B* 47 (1993) 4863.
- [71] L. Ojamäe, K. Hermansson, R. Dovesi, C. Roetti, V.R. Saunders, *J. Chem. Phys.* 100 (1994) 2128.
- [72] J.M. Besson, Ph. Pruzan, S. Klotz, G. Hamel, B. Silvi, R.J. Nelves, J.S. Loveday, R.M. Wilson, S. Hull, *Phys. Rev. B* 49 (1994) 12540.
- [73] M. Benoit, M. Bernasconi, P. Focher, M. Parrinello, *Phys. Rev. Lett.* 76 (1996) 2934.
- [74] T. Hashimoto, S. Sugawara, Y. Hiwatari, *J. Phys. Chem. B* 101 (1997) 6293.
- [75] M. Bernasconi, P.L. Silvestrelli, P. Parrinello, *Phys. Rev. Lett.* 81 (1998) 1235.
- [76] M. Benoit, D. Marx, M. Parrinello, in: U. Landmann (Ed.), *Computational Materials Science*, Elsevier, Amsterdam, 1998, pp. 88–93.
- [77] M. Benoit, D. Marx, M. Parrinello, *Nature* 392 (1998) 258.
- [78] P.G. Johansson, V. Schäferjohann, S. Kapphan, *J. Phys. Condens. Matter* 11 (1999) 583.
- [79] R.J. Nelves, J.S. Loveday, R.M. Wilson, J.M. Besson, Ph. Pruzan, S. Klotz, G. Hamel, S. Hull, *Phys. Rev. Lett.* 71 (1993) 1192.
- [80] R.J. Nelves, J.S. Loveday, W.G. Marshall, J.M. Besson, S. Klotz, G. Hamel, *Rev. High Pressure Sci. Technol.* 7 (1998) 1138.
- [81] J.S. Loveday, R.J. Nelves, W.G. Marshall, J.M. Besson, S. Klotz, G. Hamel, *Physica B* (1998) 240.
- [82] J.M. Besson, *Image de la Physique*, CNRS, Paris, 1986, p. 41.
- [83] A. Werner, H.D. Hochheimer, *Phys. Rev. B* 25 (1982) 5929.
- [84] S.D. Hamann, M. Linton, *Trans. Faraday Soc.* 62 (1966) 2234.
- [85] S.D. Hamann, M. Linton, *Trans Faraday Soc.* 65 (1969) 2186.
- [86] W.B. Holzapfel, *J. Chem. Phys.* 50 (1969) 4424.
- [87] A.C. Mitchell, W.J. Nellis, *J. Chem. Phys.* 76 (1982) 6273.
- [88] M. Sakashita, H. Yamawaki, H. Fujihisa, K. Aoki, *Phys. Rev. Lett.* 79 (1997) 1082.